

Non-Inductive Formation of Spherical Tokamak Plasmas by ECH on CPD

Tomokazu YOSHINAGA, Kazuaki HANADA¹⁾, Kohnosuke SATO¹⁾, Hideki ZUSHI¹⁾, Kazuo NAKAMURA¹⁾, Hiroshi IDEI¹⁾, Mizuki SAKAMOTO¹⁾, Yousuke NAKASHIMA²⁾, Makoto HASEGAWA¹⁾, Yuta HIGASHIZONO¹⁾, Shoji KAWASAKI¹⁾, Hisatoshi NAKASHIMA¹⁾, Aki HIGASHIJIMA¹⁾, Rajendraprasad BHATTACHARYAY³⁾, Kosuke DONO³⁾, Hiroshi HONMA³⁾, Masaki ISHIGURO³⁾, Takashi SAKIMURA³⁾, Tomofumi RYOKAI³⁾ and Toshimasa MIYAZAKI³⁾

National Institute for Fusion Science, Gifu 509-5292, Japan

¹⁾*Research Institute for Applied Mechanics, Kyushu University, Fukuoka 816-0811, Japan*

²⁾*Plasma Research Center, University of Tsukuba, Ibaraki 305-8577, Japan*

³⁾*Interdisciplinary Graduate School of Engineering Sciences, Kyushu University, Fukuoka 816-0811, Japan*

(Received: 1 September 2008 / Accepted: 22 January 2009)

Non-inductive plasma current generation and the resultant formation of closed magnetic surfaces have been achieved by electron-cyclotron-heating (ECH) in the compact plasma-wall-interaction experimental device (CPD). The rapid increase of plasma current called “current jump”, which connects externally applied open-field configuration with closed-field equilibrium, has been observed under relatively high vertical fields. By comparing normal X-mode injection and co-directional O-mode injection, the critical currents, at which current jump starts and stops, are found to be independent of the incident wave mode. However, under open-field configuration before the current jump, co-directional O-mode is more effective than normal X-mode in generating plasma currents.

Keywords: spherical torus, non-inductive current drive, electron cyclotron heating

1. Introduction

In tokamak systems, toroidal plasma currents are indispensable in the formation of nested magnetic surfaces for plasma confinement. These plasma currents are usually generated by ohmic heating (OH), which uses toroidal electric fields (E_T) induced by the central solenoids (CSs). In fusion devices, however, E_T will be small and might be insufficient to start-up plasma currents because those coils should be superconducting coils (e.g. ≤ 0.3 V/m in ITER [1]). Recently, various alternative current initiation methods are being studied, especially in spherical tokamak (ST) devices since the central space of STs are tightly limited. Moreover, if non-inductive current start-up scenarios can be fully established, ST reactors without CSs, which is advantageous to realize high β , high bootstrap current fraction, compact shape and low cost, might be constructed.

Electron cyclotron heating and current drive (ECH/ECCD), which will be used to assist OH start-up for reliable avalanche breakdown in ITER [1], is one of the possible candidates for the current initiation method. In many devices, including conventional tokamaks, generation of toroidal plasma current has been observed in EC-heated plasmas during the breakdown phase [2, 3, 4]. The non-inductive current generated in the open field configurations is understood as

a pressure-driven current, which is a short-circuit current along the tilted magnetic field lines to cancel the vertical electric field generated by the toroidal drifts [3, 5]. Since this current decreases with the vertical magnetic field (B_v), the pressure-driven mechanism is insufficient to form the nested magnetic flux surfaces by itself especially under high B_v fields. Recently, however, it was found that this initial current generation phase is followed by the “current jump” phase, which is the rapid current rise resulting in the field transition from open configuration to closed flux surface configuration [5, 6]. Moreover, additional current ramp-up by increasing B_v has been achieved after current jump [7, 8].

The current jump and the succeeding current ramp-up have been demonstrated most successfully in the LATE device, which has a slim center post even among the STs (the 0.114 m diameter center post in the 1 m diameter vacuum vessel) [8]. On the other hand, the other similar scale STs with CSs such as CPD, TST-2 [9] and CDX-U [3], have the center posts which are twice as large as LATE (~ 0.25 m) in similar size vacuum vessels ($\lesssim 1.4$ m). Wider center post limits the aspect ratio of the plasma loop to a higher value. Since no current jump has been observed in the conventional tokamaks, it is not certain whether the ECH-based current start-up scenario via current jump can be applicable to such STs with somewhat higher aspect ratios. Recently, the current jump phenomena

author's e-mail: yoshinaga.tomokazu@LHD.nifs.ac.jp

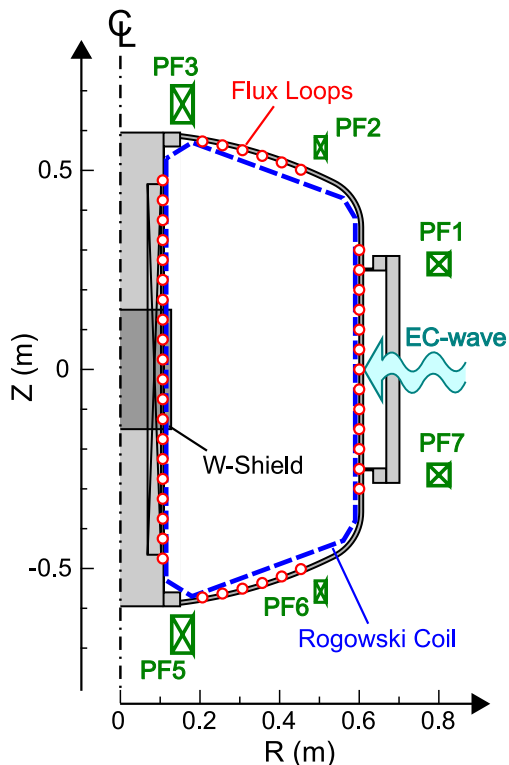


Fig. 1 The CPD device.

has been observed under small B_v ($\lesssim 10$ G) and low microwave power ($P_{rf} \lesssim 5$ kW) injection in TST-2 [6]. However, it seems still too early to conclude that the ECH-based scenario is well reliable, since the B_v is limited to a very small range. In order to confirm this, ECH has been applied to CPD under higher B_v ($\lesssim 50$ G) by using higher P_{rf} ($\lesssim 60$ kW). The experimental results showed that the current jump can occur also in CPD and suggested that the current start-up by ECH/ECCD may be applicable to some extent. The dependencies of the current jump phenomena on the microwave power, the injection modes, and the vertical fields are also investigated. This paper describes the experimental setup in section 2, experimental results in section 3, discussions in section 4, and summary in section 5.

2. Experimental Apparatus

Figure 1 shows the schematic of CPD. Both of the inner diameter and the height of the stainless-steel vacuum vessel are 1.2 m. The center post, whose outer diameter is 0.22 m, encloses four turns of toroidal field coils and CS. Around the mid-plane, it is covered by four pieces of quarter round tungsten-coated shield, the outer diameter and the height of which is ~ 0.255 m and 0.3 m, respectively. Three sets of outer poloidal field coils (PF17, PF26 and PF35), which can be driven separately by the pre-programmed power sources, are used. The CS is not used in this experi-

ment. Microwave at 8.2 GHz from 8 klystrons is transmitted separately to the eight rectangular waveguide antennas and injected from the weak field side. Four antennas are placed for the injection of the wave vector normal to the field line and of the electric field inclined at 22.5° to the vertical (Z) axis (we call this mode “X-mode” for simplicity). The remaining four antennas are used for the injection of the “O-mode”, which has the electric field orthogonal to the X-mode. The waves in O-mode can be injected tangentially by the movable mirrors. The working gas is hydrogen.

Plasma current is measured by the Rogowski coil, and magnetic flux profiles are estimated from the 45 flux loop signals by using a similar technique to that mentioned in [10]. In addition, a lithium (Li) sheet beam imaging technique for density profile measurement [11, 12], a filtered high-speed (1 ms) camera, and an ultra-high-speed ($25 \mu\text{s}$) camera are used to monitor the plasma shapes.

3. Experimental Results

Figure 2 (a)-(b) shows time evolutions of a typical current jump discharge under a weakly mirror-shaped steady vertical field at $B_v = 39$ G and n (decay index) = 0.1 (both at the vessel center, $R = 0.33$ m) as shown in Fig. 2 (d). During the weak microwave ($P_{rf} \sim 1$ kW) injection before $t = 0.12$ s under the filling gas pressure at $\sim 10^{-3}$ Pa, cylindrical plasma is generated on the fundamental EC resonance (ECR) layer for a 8.2 GHz microwave ($B = 0.29$ T) at $R = 0.19$ m. As P_{rf} increases after $t = 0.12$ s [Fig. 2 (a)], plasma current (I_p) also increases gradually with P_{rf} and reaches 1.2 kA under $P_{rf} = 50$ kW at $t = 0.154$ s, as shown in Fig. 2 (c). Then, the current jump phase is turned on and I_p rapidly increases up to 2 kA in ~ 3 ms, and keeps this value until P_{rf} starts to decrease at $t \sim 0.32$ s. Magnetic analysis shows that the externally applied open magnetic field shown in Fig. 2 (d) changes into the upward shifted closed flux configuration as shown in Fig. 2 (e) in this current jump phase. The aspect ratio of the last closed flux surface (LCFS) is $R_0/a \sim 2$, while the major radius (R_0) and the minor radius (a) are $R_0 \sim 0.2$ m and $a \sim 0.1$ m, respectively. This transition of field topology via current jump can be verified by both high-speed camera images and sheet Li beam images [12]. Moreover, sheet Li beam diagnostics suggests that the electron density exceeds the cutoff density for a 8.2 GHz EC-wave ($8.3 \times 10^{17} \text{ m}^{-3}$) after current jump [12]. This suggests that the electron-Bernstein wave heating might be taking place in this phase.

The result that the current jump has been observed in CPD as well as in LATE and in TST-2 demonstrates that this phenomenon can occur com-

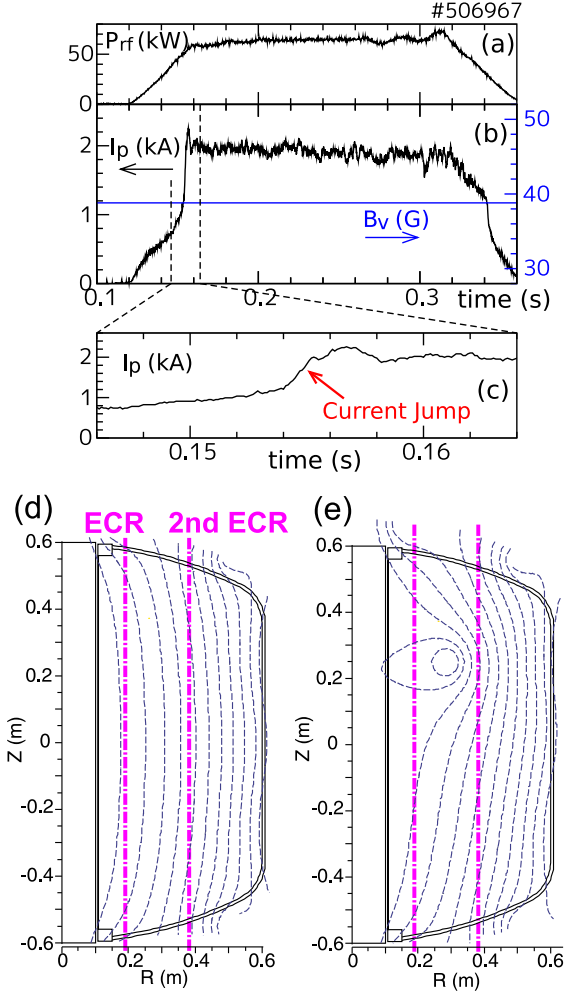


Fig. 2 Typical discharge with current jump. (a) P_{rf} , (b) I_p and B_v , (c) enlarged I_p around current jump, (d) external poloidal field, (e) closed-flux configuration after current jump ($t \sim 0.18$ s).

monly in STs. A larger aspect ratio ($R_0/a \sim 2$) than the typical case in LATE ($R_0/a \sim 1.4$) [8] can be allowed as well as the twice wider center post.

By the careful wall conditionings and the optimizations of the filling gas pressure, current jump can be observed at a lower P_{rf} than the case in Fig. 2, even under the same B_v condition. In Fig. 3, the transient values of I_p during the initial phase of such optimized discharges are plotted against the transient P_{rf} in normal X-mode and co-directional O-mode. Since the increasing rates of P_{rf} ($dP_{rf}/dt \lesssim 1$ kW/ms) are considered to be very small by considering the energy confinement time of CPD plasmas ($\lesssim 10 \mu\text{s}$), the relationships can be understood as a steady state dependencies. These characteristics do not depend on the increasing rate of P_{rf} . The values of I_p before current jump show the monotonic increases with P_{rf} in both modes. Since I_p in this phase is considered to be the pressure driven current, the increase of I_p should correspond to the increase of plasma pressure with

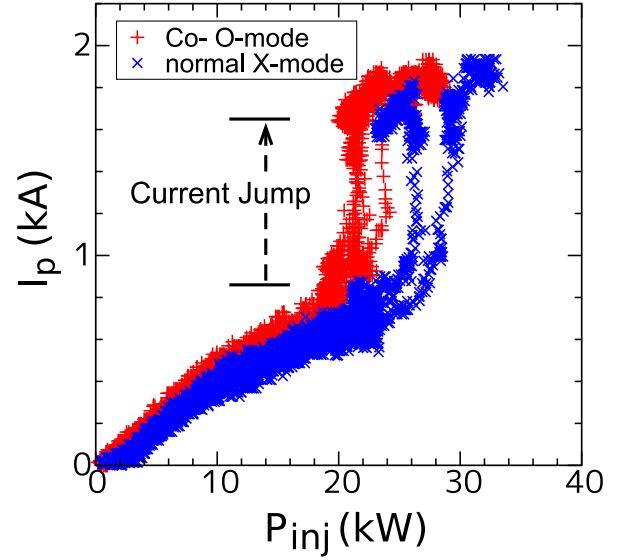


Fig. 3 $I_p - P_{rf}$ characteristics for co-directional O-mode injection and normal X-mode injection. $B_v = 39$ G, $n = 0.1$ at $R = 0.33$ m.

P_{rf} . While the co-directional O-mode injection seems to be slightly more effective than the normal X-mode injection, the current generation efficiencies of those two injection modes are quite similar before current jump. However, there is a clear difference between these modes in the current jump phase. The threshold P_{rf} at which the current jump starts is $P_{rf} \sim 20 - 23$ kW in co-directional O-mode, while it is $\sim 26 - 29$ kW in normal X-mode. Since I_p before and after current jump seems to be independent of the injection modes as the TST-2 results [6], the essential parameter for the occurrence of the current jump should be I_p itself, which determines the critical poloidal configuration by the self field. The difference between the two injection modes would be related to the ECH efficiency to raise the electron pressure and the pressure-driven I_p to some threshold level which is needed to start the current jump.

In Fig. 4, I_p with and without current jump are plotted against B_v for various discharges with various $P_{rf} \lesssim 60$ kW. Clear current jumps can be observed under relatively high B_v fields ($\gtrsim 30$ G). Higher I_p ($\gtrsim 2$ kA) can only be achieved via current jump under this B_v range, while I_p saturates at ~ 1.7 kA without the current jump. This shows that the current jump is essential to obtain the closed-field equilibrium at higher I_p under higher B_v . In contrast, under lower B_v ($\lesssim 30$ G) fields, current jump is not observed clearly. In such discharges I_p increases slowly with increase of P_{rf} as shown in Fig. 5 (a) and (b), and reaches to a certain level that is proportional to B_v . Since the ratio of I_p to B_v without clear current jumps is similar to that with current jumps ($dI_p/dB_v \sim 0.08$ kA/G), closed-flux equilibria may be formed even without cur-

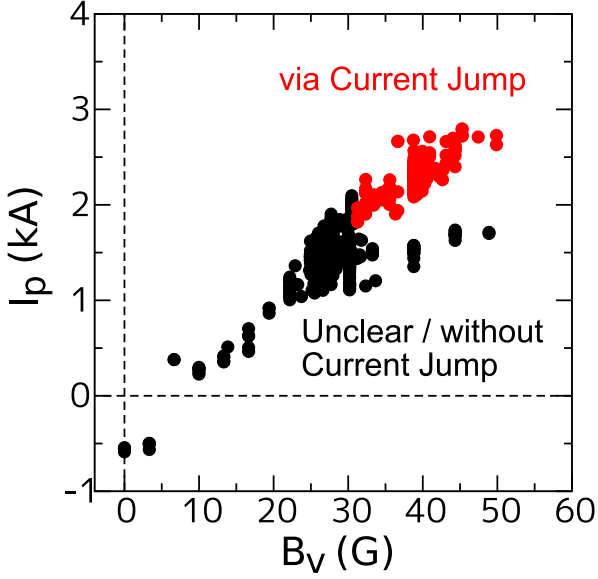


Fig. 4 I_p as a function of B_v under $P_{rf} \lesssim 60$ kW.

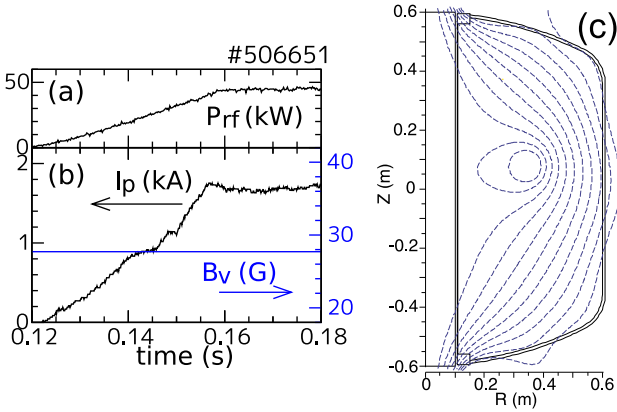


Fig. 5 Discharge without current jump under lower B_v . (a) P_{rf} , (b) I_p and B_v , and (c) poloidal flux structure estimated at the flattop. $B_v = 28$ G with $n = 0.34$ (both at $R = 0.33$ m) is applied.

rent jump as well as in the current jump discharges. However, this type of discharge is less effective in P_{rf} . In the discharge shown in Fig. 5 $P_{rf} \sim 40$ kW must be injected to achieve $I_p \sim 2$ kA even under the optimized circumstances, while in the current jump discharge the same I_p can be achieved by $P_{rf} \lesssim 30$ kW even within the less effective normal X-mode.

There is an offset of $B_v \sim 5$ G in the $I_p - B_v$ characteristics as shown in Fig. 4. Related to this, the upward shift of the LCFS structure is seen as shown in Fig.2 (d), while it is suppressed under the B_v field with higher n as shown in Fig.5 (c). These might suggest the existence of some error fields in vertical direction.

4. Discussion

To hold a toroidal plasma loop in equilibrium the following relationship should be satisfied:

$$B_v = \frac{\mu_0 I_p}{4\pi R} \left(\ln \frac{8R_0}{a} + \frac{l_i}{2} - \frac{3}{2} + \beta_{p,eq} \right), \quad (1)$$

where l_i is the internal inductance and $\beta_{p,eq}$ is the poloidal beta for equilibrium of the plasma loop. The linear increase of I_p with B_v in the rate of $dI_p/dB_v \sim 0.08$ kA/G shown in Fig. 4 suggests that a certain constant $\beta_{p,eq} \sim 0.7$ on the assumption of $R_0 \simeq 0.2$ m, $a \simeq 0.1$ m and $l_i \sim 1$ for plasma loop. By assuming the bulk electron density $n_e \sim 1 \times 10^{18} \text{m}^{-3}$ and the bulk electron temperature $T_e \sim 10$ eV for typical parameters in CPD, the bulk electrons' β_p scales as $\beta_{p,bulk} = 8\pi^2 a^2 n_e T_e / \mu_0 I_p^2 \sim 1 \times I_p^{-2}$ (I_p in kA), and becomes 1 when $I_p = 1$ kA. In order that the equilibrium condition under higher B_v may be satisfied only by the bulk electrons, the relationship that $\beta_{p,bulk} = \beta_{p,eq} \sim 0.7$ must be satisfied. This means that the bulk electron pressure should rise with the square of B_v as well as I_p , which is unlikely in CPD plasmas with the poor confinement times ($\lesssim 10 \mu\text{s}$). The contribution from the tail electrons ($\beta_{p,tail}$), which are considered as the current carriers during and after current jump phase [5, 7], is therefore suggested to exist to keep the constant $\beta_{p,eq}$ especially under higher B_v fields in place of $\beta_{p,bulk}$, which would decrease with B_v . This is also suggested by the directional Langmuir probe experiments in CPD, in which the existence of high-energy electrons is suggested only in the direction of positive I_p generation.

5. Summary

Non-inductive current generation and the formation of the closed-flux equilibrium have been achieved via current jump by using a 8.2 GHz EC-wave on CPD. The current jump can be obtained under higher B_v ($\gtrsim 30$ G), while I_p slowly increases with P_{rf} under lower B_v ($\lesssim 30$ G). The values of I_p before and after current jump does not depend on the injection mode, while the threshold P_{rf} at which the current jump starts is lower in co-directional O-mode than in the normal X-mode. These results suggest that the critical parameter for current jump is I_p itself, and therefore the poloidal field structure. The injection modes are related to the current generation efficiency in the open-field configuration.

Since the aspect ratio of the Q-shu University with Steady State Spherical Tokamak (QUEST) [13], which is the next step larger ST device, is quite similar to the aspect ratio of CPD, it can be expected that the non-inductive current start-up via current jump would be applied to the QUEST operation.

6. Acknowledgment

This work was performed with the support and under the auspices of the NIFS Collaboration Research Program (NIFS05KUTR007).

- [1] Y. Gribov *et al.*, Nucl. Fusion **47**, S385 (2007).
- [2] S. Kubo *et al.*, Phys. Rev. Lett. **50**, 1994 (1983).
- [3] C. B. Forest *et al.*, Phys. Plasmas **1**, 1568 (1994).
- [4] M. Gryaznevich *et al.*, Nucl. Fusion **46**, S573 (2006).
- [5] T. Yoshinaga *et al.*, Phys. Rev. Lett. **96**, 125005 (2006).
- [6] J. Sugiyama *et al.*, Plasma Fusion Res. **3**, 026 (2008).
- [7] M. Uchida *et al.*, IEEJ Trans. FM **125**, 914 (2005).
- [8] T. Maekawa *et al.*, Nucl. Fusion **45**, 1439 (2005).
- [9] Y. Takase *et al.*, Nucl. Fusion **46**, S598 (2006).
- [10] T. Yoshinaga *et al.*, Nucl. Fusion **47**, 210 (2007).
- [11] R. Bhattacharyay *et al.*, Phys. Plasmas **15**, 022504 (2008).
- [12] T. Kikukawa *et al.*, Plasma Fusion Res. **3**, 010 (2008).
- [13] K. Hanada *et al.*, *Proc. 22nd IAEA Fusion Energy Conf.* IAEA-CN-165/FT/P3-25, Geneva, Switzerland, 2008